

PAPER • OPEN ACCESS

## Determining the fuel ion ratio for D(T) and T(D) plasmas at JET using neutron time-of-flight spectrometry

To cite this article: B Eriksson *et al* 2022 *Plasma Phys. Control. Fusion* **64** 055008

View the [article online](#) for updates and enhancements.

### You may also like

- [Analysis of resonant fast ion distributions during combined ICRF and NBI heating with transients using neutron emission spectroscopy](#)  
C. Hellesen, M. Mantsinen, S. Conroy et al.
- [Conceptual design of the high resolution neutron spectrometer for ITER](#)  
Marek Scholz, Anders Hjalmarsson, Leszek Hajduk et al.
- [Maximizing D-T fusion power by optimising the plasma composition and beam choice in JET](#)  
Dirk Van Eester, Ernesto A Lerche, Philippe Huynh et al.



**IOP | ebooks™**

Bringing together innovative digital publishing with leading authors from the global scientific community.

Start exploring the collection—download the first chapter of every title for free.

# Determining the fuel ion ratio for D(T) and T(D) plasmas at JET using neutron time-of-flight spectrometry

B Eriksson<sup>1,\*</sup> , S Conroy<sup>1</sup>, G Ericsson<sup>1</sup> , J Eriksson<sup>1</sup> , A Hjalmarsson<sup>1</sup> , Z Ghani<sup>2</sup>, I S Carvalho<sup>2,3</sup> , I Jecu<sup>4</sup> , E Delabie<sup>5</sup> , M Maslov<sup>2</sup>, M Lennholm<sup>2</sup>, F Rimini<sup>2</sup>, D King<sup>2</sup> and JET Contributors<sup>6,7</sup>

<sup>1</sup> Department of Physics and Astronomy, Uppsala University, Uppsala SE-751 20, Sweden

<sup>2</sup> UKAEA, Culham Centre for Fusion Energy, Abingdon, United Kingdom

<sup>3</sup> Instituto de Plasmas e Fusão Nuclear, IST, Universidade de Lisboa, Lisbon, Portugal

<sup>4</sup> National Institute for Laser, Plasma and Radiation Physics, Bucharest-Magurele 077125, Romania

<sup>5</sup> Oak Ridge National Laboratory, Oak Ridge, TN 37831-6169, United States of America

<sup>6</sup> EUROfusion Consortium, JET, Culham Science Centre, Abingdon, Oxfordshire OX14 3DB, United Kingdom

E-mail: [benjamin.eriksson@physics.uu.se](mailto:benjamin.eriksson@physics.uu.se)

Received 23 November 2021, revised 23 February 2022

Accepted for publication 2 March 2022

Published 4 April 2022



CrossMark

## Abstract

The fusion fuel ion ratio,  $n_T/n_D$ , is an important plasma parameter that needs to be tuned to maximize the power of a tokamak type fusion reactor. It is recognized as a parameter required for optimizing several ITER operating scenarios, and will likely be continuously monitored in future high-performance fusion devices such as DEMO. Tritium was recently introduced in the Joint European Torus (JET) plasma for the first time since the 1997 DTE1 and 2003 TTE campaigns, enabling the possibility to investigate fuel ion ratios. We present a method for measuring  $n_T/n_D$  using neutron time-of-flight (TOF) spectrometry. By fitting the measured neutron spectral features, the relative reaction rate intensities between different ion species can be inferred, from which the fuel ion ratio can be extracted for a corresponding modeled reactivity. Unlike previous measurements of  $n_T/n_D$  using neutron spectrometry, we utilize the neutron energy continuum produced in the three-body TT reaction to determine the fuel ion ratio for plasmas with large concentrations of tritium. Furthermore, the use of neutron TOF spectrometry has never previously been demonstrated for evaluating  $n_T/n_D$ . The method is applied to TOF spectra acquired with TOFOR (JET name KM11) and shown to be consistent with the optical JET diagnostic KT5P which uses optical spectroscopy of a modified Penning gauge plasma to measure tritium and deuterium concentrations in the divertor exhaust gas.

<sup>7</sup> See the author list of Joffrin et al 2019 Nucl. Fusion **59** 112021.

\* Author to whom any correspondence should be addressed.



Original Content from this work may be used under the terms of the [Creative Commons Attribution 4.0 licence](https://creativecommons.org/licenses/by/4.0/). Any further distribution of this work must maintain attribution to the author(s) and the title of the work, journal citation and DOI.

Keywords: fuel ion ratio, neutron spectrometry, time-of-flight, TOFOR, KT5P, Penning gauge, Joint European Torus

(Some figures may appear in colour only in the online journal)

## 1. Introduction

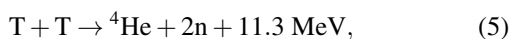
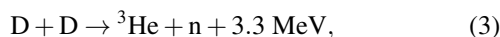
The fusion fuel ion ratio, defined as the ratio of deuterium (D) and tritium (T) number densities,  $n_T/n_D$ , is an important parameter for maintaining plasma control and performance of future fusion plasmas. The reaction rate for two ion populations with densities  $n_1$  and  $n_2$  is

$$R = n_1 n_2 \langle \sigma v \rangle_{12}, \quad (1)$$

where the reactivity

$$\langle \sigma v \rangle_{12} = \int f_1(\vec{v}_1) f_2(\vec{v}_2) \sigma(v) v d\vec{v}_1 d\vec{v}_2, \quad (2)$$

is given by integrating over the velocity distributions ( $f_1$  and  $f_2$ ), the fusion reaction cross section ( $\sigma$ ) and the relative velocity ( $v = |\vec{v}_2 - \vec{v}_1|$ ). If we replace the subscripts 1 and 2 with D and T, we find a maximum in the reaction rate for equal amounts of deuterium and tritium ( $n_T/n_D = 1$ ), which shows the significance of the fuel ion ratio for maximizing the fusion power.  $n_T/n_D$  has been identified as an important parameter to monitor at ITER for several operating scenarios, with a time resolution of 100 ms, a spatial resolution of  $a/10$ , an accuracy of 20%, and for a range of  $0.01 < n_T/n_D < 10$  [1], and will likely also be continuously monitored in future high-performance fusion devices such as DEMO. The fuel ion ratio has, in addition to neutron spectrometry, previously been suggested to be measured through collective Thomson scattering and charge exchange recombination spectrometry [1, 2]. In preparation for the DTE2 campaign planned for the end of 2021, tritium was added to the Joint European Torus (JET) plasma with varying concentrations for the first time since the deuterium-tritium experimental campaign (DTE1) in 1997 and the trace tritium experimental campaign (TTE) in 2003. In the work presented here,  $n_T/n_D$  is determined in trace deuterium, T(D), and trace tritium, D(T), JET plasmas using neutron time-of-flight spectrometry based on simulations and modeling techniques developed previously in e.g. [3–5]. Three neutron-producing fusion reactions are of interest here, namely



where the average energy obtained by the neutron in (3) and (4) is 2.45 MeV and 14.1 MeV respectively. The TT reaction in (5) is a three-body reaction, yielding a continuum of neutron energies ranging between 0 and 10 MeV. The reaction rates

for DD and TT reactions can be set up similarly to (1), and the contribution of neutrons from the different reactions can be inferred from the measured neutron spectrum.

## 2. Experimental

Four JET discharges were selected for the fuel ion ratio analysis. Plasma parameters as a function of time for the given discharges are shown in figure 1. The rows of the figure correspond to (1) the neutron rate, (2) the gas injection rate (number of molecules per second) and the corresponding gas type, (3) the total neutral beam injection (NBI) power and beam ion type, (4) the plasma electron density, and (5) the plasma electron temperature. The left column shows two D(T) plasmas with JET Pulse Number (JPN) 98043 and 98044. These correspond to discharges devoted to calibration of various neutron diagnostics performed in late 2020, in which small amounts of T gas were injected into a D plasma with D NBI heating. The lines for the T gas injection for 98043 and 98044 nearly overlap in the figure. The right panel displays two H(T) plasmas with JPN 99093 and 99134 corresponding to T NBI conditioning discharges from early 2021. Hydrogen gas was injected into the plasma before and, to an extent, during the discharge time window shown in the figure. Ohmic and T NBI heating was utilized. The plasmas for these two shots consist of a majority of hydrogen (approximately 60%–80% throughout the discharge), however, since there is no source of injected D, tritium is the dominating ion species with respect to  $n_T/n_D$ , hereafter these will therefore be referred to as T(D) plasmas.

### 2.1. TOFOR

The time-of-flight (TOF) neutron spectrometer TOFOR [6] (JET name KM11) is optimized for high count rates and performing neutron emission spectrometry on, in the first hand, D plasmas. However, due to its broadband capabilities, it is to a degree possible to perform the analysis on other fuel compositions as well. The spectrometer consists of two sets of plastic scintillators, the first set providing a start signal, and the second a stop signal for the TOF measurements. TOFOR has a vertical sight-line through the core of the JET plasma, shown in figure 2. TOFOR's neutron spectral measurements are consequently line-integrated averages, heavily weighted towards the plasma core, due to the centrally peaked distribution of the neutron emission profile [7, 8].

## 3. Method

The measured neutron TOF (energy) spectrum depends on the fuel composition (here corresponding to  $n_T/n_D$ ), the applied fuel heating scheme, and the sight-line of the diagnostic

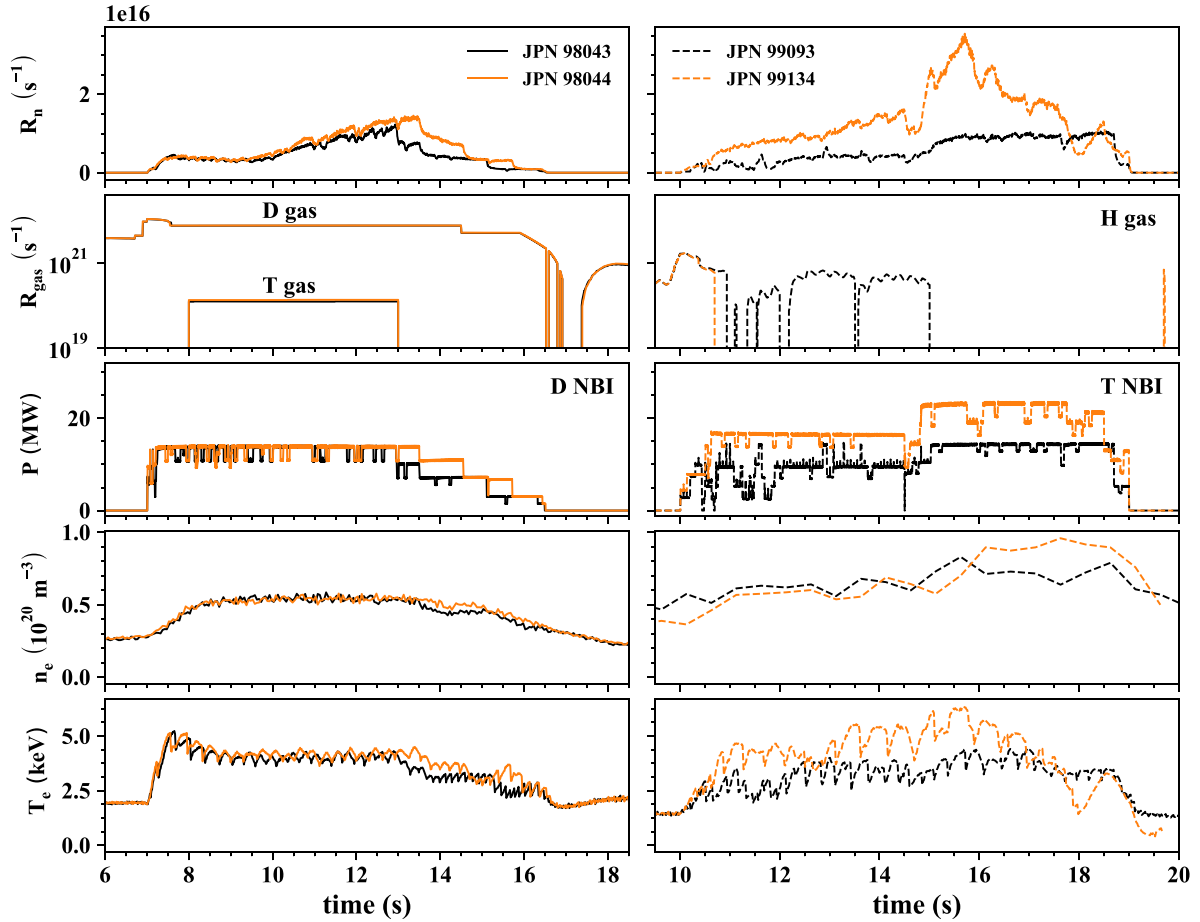


**Figure 1.** Plasma discharge parameters for JET pulse number (JPN) 98043 and 98044 (left column), and JPN 99093 and 99134 (right column).

performing the measurement, as well as an unavoidable background component from random coincidences (coming from the start and stop detectors triggering on different uncorrelated events within the allowed TOF time window) and scattering in JET materials. Two TOF spectra, measured by TOFOR, for the two JET discharges with JPN 98044 and 99093, are shown in figure 3. In panel (a) the plasma consists of a majority of deuterium with a low level of tritium gas injection. The fuel was heated through Ohmic heating and NBI with D particles. Three main features are visible in the spectrum: (1) a peak around  $t_{\text{TOF}} = 4$  ns corresponding to gamma rays ( $\gamma$ ) (which due to the constant speed of light have a constant flight time irrespective of  $\gamma$  energy), (2) a DT neutron peak around  $t_{\text{TOF}} = 27$  ns corresponding to 14.1 MeV neutrons, and (3) a DD neutron peak around  $t_{\text{TOF}} = 67$  ns corresponding to 2.45 MeV neutrons. In panel (b) the plasma consists of a majority of  $^1\text{H}$ , a minority of T, and trace amounts of D, and was heated using Ohmic heating and a tritium NBI. Similar features are visible in the spectrum, however, the DD peak has been replaced by neutrons from the TT reaction. In addition to these features, random coincidences give rise to a flat background across the full TOF spectrum, present regardless of the fuel composition. The average background component due to random coincidences can be calculated by extending the TOF window to negative flight times, exemplified from  $-20$  to  $0$  ns in figure 3, where nothing

but random coincidences is expected. The average of the negative flight times is then used as a fixed component in the fitting procedure, and subsequently subtracted from the positive flight time region when plotting the spectrum. Finally, energy degraded neutrons (caused by scattering in various JET components and building materials) contribute to the spectra on the low energy (high  $t_{\text{TOF}}$ ) side of their respective direct, full energy peaks. Consequently, energy degraded neutrons from the DT peak may affect the visibility of the DD and TT peaks. If the reaction rate in the plasma is to a large degree dominated by DT reactions, typically for ion ratios in a broad range on the order of  $0.2 \lesssim n_{\text{T}}/(n_{\text{T}} + n_{\text{D}}) \lesssim 0.8$ , the DD and TT contributions to the spectrum can be completely drowned out by such energy degraded DT neutrons.

### 3.1. Spectral features

The various heating schemes applied to the plasma give rise to separate ion populations, each with its own characteristic energy distribution. These, in turn, yield distinct features in the neutron energy spectrum with different relative intensities. Normally, for an NBI heated JET plasma, the dominating contribution to the neutron spectrum consists of beam-thermal (bt) reactions, i.e. reactions between NBI accelerated fuel ions and thermal ions. Additionally, there is a contribution

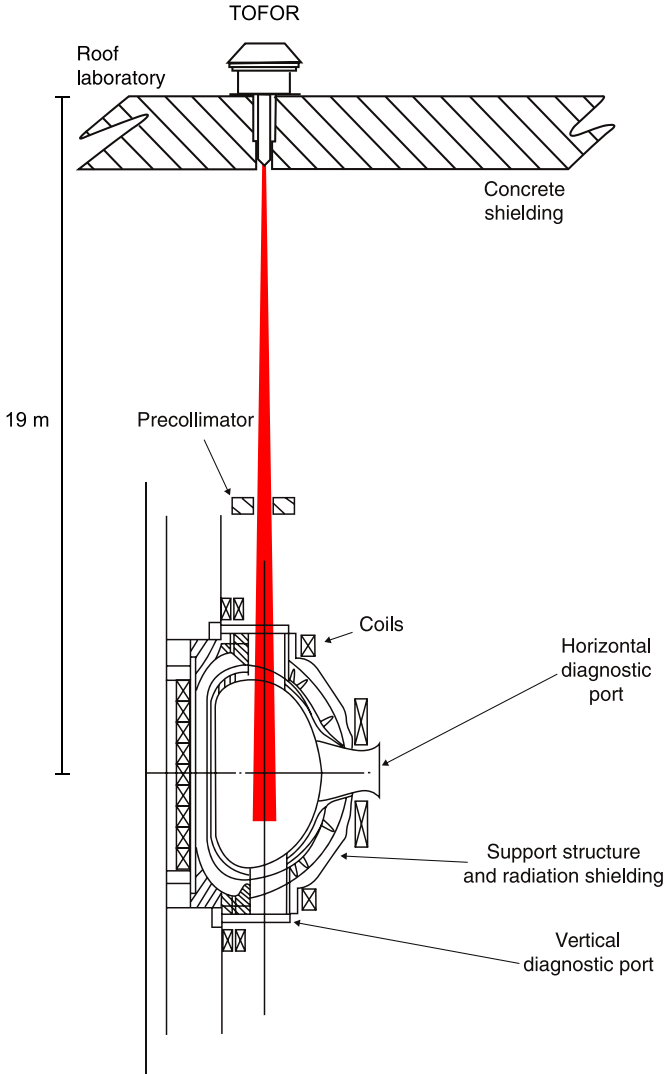


**Figure 2.** Sight-line of TOFOR relative to a poloidal cut of the JET machine.

from thermal (th) reactions (reactions between two particles from the thermal ion population). Finally, neutrons can scatter in various JET components into the TOFOR sight-line. In figure 4, these three components have been used to describe (fit) the DD peak of JPN 98044 for the discharge time windows 7–8 s (left panel) and 12–13 s (right panel). The fitting procedure for the thermal and beam-thermal components follow four steps: (1) the ion velocity distributions of the reacting particles are modeled, (2) the corresponding neutron energy distributions are determined, (3) the corresponding neutron TOF spectrum is estimated by folding the neutron energy distribution with the instrumental response function, and (4) the calculated TOF spectrum is fit to the data.

**3.1.1. Thermal-thermal component.** The thermal ion velocity distribution is modeled with the assumption that an ion population in thermal equilibrium conforms to a Maxwellian energy distribution. This has been shown to yield a neutron spectrum accurately resembling a Gaussian distribution [8]

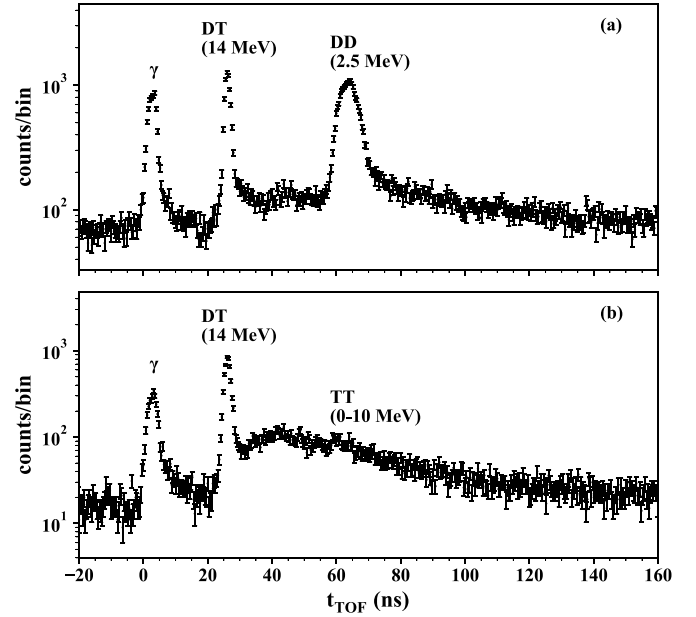


**Figure 3.** Time-of-flight spectra measured over the full JET discharge duration for (a) JPN 98044 and (b) JPN 99093.

$$f(E_n) = \frac{1}{W\sqrt{\pi}} \exp\left(-\frac{(E_n - \langle E_n \rangle)^2}{W^2}\right), \quad (6)$$

$$W = \sqrt{\frac{4m_n \langle E_n \rangle T_i}{m_n + m_{\text{He-3}}}}, \quad (7)$$

where the width of the distribution,  $W$ , depends on the average neutron energy  $\langle E_n \rangle$ , the reaction product masses  $m_n$  and  $m_{\text{He-3}}$  and, finally, the ion temperature  $T_i$ . Here, the assumption  $T_i = T_e$  is made. Typically, at JET, the average ion temperature is higher than the average electron temperature. However, since the DD peak in the spectrum is to a large degree dominated by the beam-thermal DD component (green dash-dotted line in figure 4), a slight change in the width of the thermal component (magenta line) will not affect the overall fit to a large extent.

**3.1.2. Beam-thermal component.** The NBI ion velocity distribution is modeled using a one-dimensional Fokker–Planck equation [9]

$$\frac{\partial f}{\partial t} = \frac{1}{v_i^2} \frac{\partial}{\partial v_i} \left[ -\alpha v_i^2 f + \frac{1}{2} \frac{\partial}{\partial v_i} (\beta v_i^2 f) \right] + S(v_i) + L(v_i), \quad (8)$$

where  $\alpha$  and  $\beta$  are Coulomb coefficients derived by Spitzer [10],  $S(v_i)$  is a source term for injected NBI particles and  $L(v_i)$  is a loss term for removing thermalized ions. A steady state solution of (8) can be found by setting  $\partial f/\partial t = 0$ , and used to calculate the expected ion velocity distribution of injected NBI ions slowing down in a thermal ion population. From the NBI and thermal distributions, the corresponding neutron energy spectrum can be estimated and, after folding with the instrumental response function, used in the fit to the TOF spectrum. In figure 4, the analysis is performed using a D NBI with an

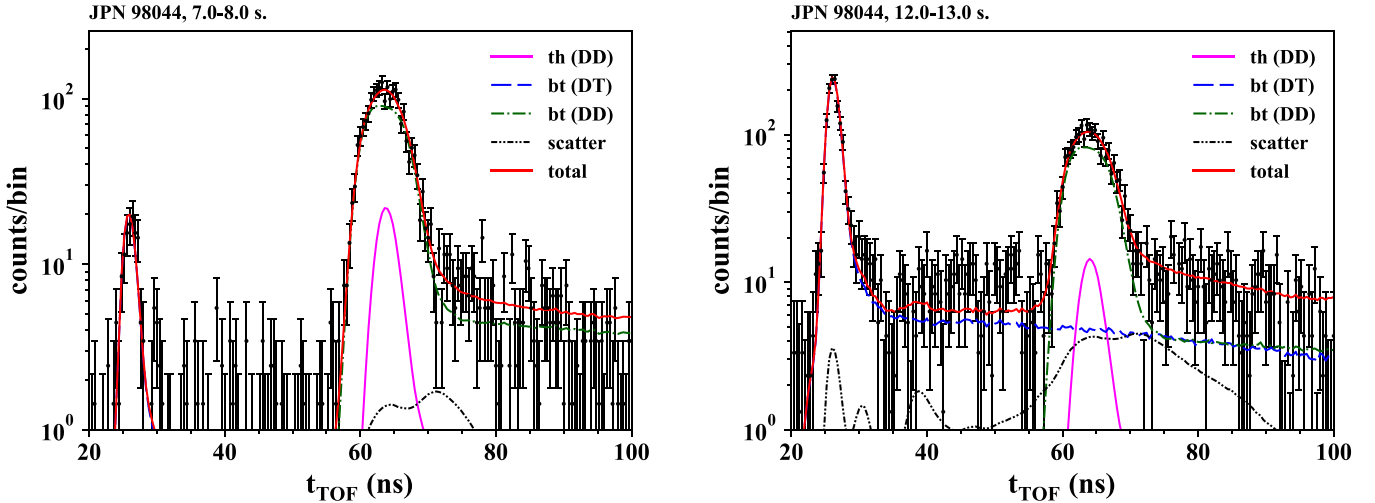


**Figure 4.** TOF spectra of JPN 98044 measured between 7–8 s (left panel) and 12–13 s (right panel) of the discharge. Four components, described in section 3, are fit to the spectra. The beam-thermal DT (blue dashed line) and total (red line) components overlap in the left panel. The uniform component due to random coincidences has been subtracted in the figure.

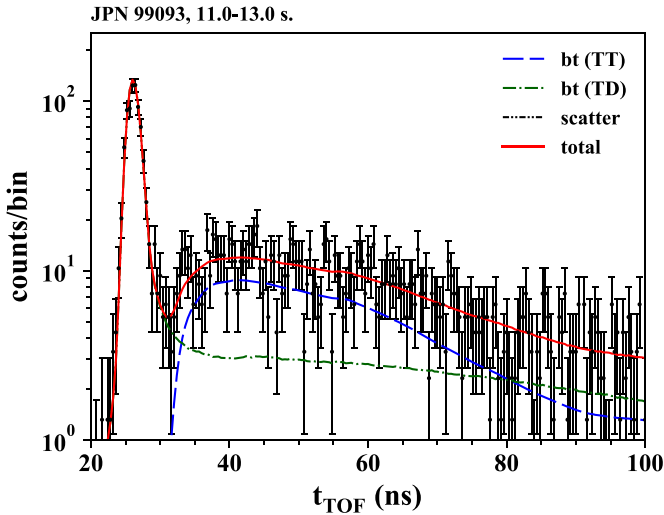


**Figure 5.** TOF spectrum of JPN 99093 measured between 11–13 s of the discharge. Three components, described in section 3, are fit to the spectrum. The background due to random coincidences has been subtracted in the figure.

injection energy of 100 keV, slowing down in a D plasma, and interacting with a thermal D population (yielding the green dash-dotted line) and a thermal T population (yielding the blue dashed line). Due to the limited resolution of TOFOR at higher energies (lower flight times), the DT peak (at 27 ns) cannot be resolved in the same way as the DD peak. Consequently, the DT peak is fit using a pure beam-thermal component. A similar analysis can be performed for the T(D) plasmas, as exemplified in figure 5. Since the majority of the plasma, in this case, consists of  $^1\text{H}$ , the tritium NBI velocity distribution is calculated using (8) for a T NBI with an injection energy of 100 keV, slowing down in a  $^1\text{H}$  plasma, and interacting with a thermal T population (giving rise to the blue dashed line) and a thermal D population (producing the green dash-dotted line).

**3.1.3. Scattered component.** The scattered neutron energy component is evaluated by multiplying the neutron energy spectrum calculated previously (beam-thermal and thermal-thermal components) with a simulated scatter matrix [11] which tells us which fraction of plasma core neutrons of a given energy is expected to scatter into the TOFOR sight-line. The scattered contribution, folded with the instrumental response function, is shown in figure 4 as the black dash-dot-dotted line. The contribution from the scatter component is too small to be visible for the given scale in figure 5.

To determine the fuel ion ratio,  $n_{\text{T}}/n_{\text{D}}$ , we apply the reaction rate equation from (1), separating the different relevant components contributing to the TOF spectrum. The applied methods for determining the ion ratio are described for a D(T) plasma and a T(D) plasma in sections 3.2 and 3.3 below.

### 3.2. Trace tritium plasma

For the D(T) plasma shown in panel (a) of figure 3, the reaction rate of the two components are

$$R_{\text{bt,DT}} = n_{\text{D}_{\text{NBI}}} n_{\text{T}} \langle \sigma v \rangle_{\text{bt,DT}}, \quad (9)$$

$$R_{\text{bt,DD}} = n_{\text{D}_{\text{NBI}}} n_{\text{D}} \langle \sigma v \rangle_{\text{bt,DD}}, \quad (10)$$

where bt (beam-thermal) signifies interactions between the NBI accelerated ion population and the thermal population, and  $n_{\text{D}_{\text{NBI}}}$  is the particle number density of the beam ions. The reactivities are calculated by solving the corresponding integrals from (2) where the velocity-dependent fusion cross section of the reaction is multiplied by the velocity distribution estimated using the one-dimensional Fokker–Planck equation mentioned earlier. By dividing (9) by (10) and rearranging we obtain the fuel ion ratio

$$\frac{n_{\text{T}}}{n_{\text{D}}} = \frac{R_{\text{bt,DT}} \langle \sigma v \rangle_{\text{bt,DD}}}{R_{\text{bt,DD}} \langle \sigma v \rangle_{\text{bt,DT}}}, \quad (11)$$

where the ratio  $R_{\text{bt,DT}}/R_{\text{bt,DD}}$  is estimated using the fits to the corresponding TOF components, examples of which are shown in figure 4.

### 3.3. Trace deuterium plasma

Similarly, for the T(D) plasma shown in panel (b) of figure 3, the reaction rates for the TD component (here labelled TD to signify that T is the NBI accelerated ion) and the TT component are given by

$$R_{\text{bt,TT}} = n_{\text{T,NBI}} n_{\text{T}} \langle \sigma v \rangle_{\text{bt,TT}}, \quad (12)$$

$$R_{\text{bt,TD}} = n_{\text{T,NBI}} n_{\text{D}} \langle \sigma v \rangle_{\text{bt,TD}}, \quad (13)$$

where the reactions are dominated by NBI T ions with thermal D and T populations. By dividing (12) by (13), we find

$$\frac{n_{\text{T}}}{n_{\text{D}}} = \frac{R_{\text{bt,TT}} \langle \sigma v \rangle_{\text{bt,TD}}}{R_{\text{bt,TD}} \langle \sigma v \rangle_{\text{bt,TT}}}, \quad (14)$$

where  $R_{\text{bt,TT}}/R_{\text{bt,TD}}$  is estimated using the fitting procedure described above, and exemplified in figure 5 for an integrated discharge time window of 11–13 s.

## 4. Results

The results from the analysis, performed for a number of discharge time intervals, are shown in tables 1 and 2. The same fuel ion ratios are also presented in figures 6 and 7 where the points correspond to the center of the given time intervals. The start and end time of the tritium gas puffing is indicated with the dashed black lines in figure 6. The fuel ion ratio measured by the JET diagnostic KT5P is shown in the same figures as the dashed orange lines. KT5P is an optical diagnostic which measures the light generated through excitations of neutral deuterium and tritium in a Penning gauge sampling the sub-divertor region [12]. The intensity of the Balmer  $\alpha$  lines from  $\text{D}_2$  and  $\text{T}_2$  is directly proportional to the concentration of the different hydrogenic isotopes in the divertor exhaust gas [13]. The KT5P optical spectroscopy signal provides measurements on a time basis of 0.05 s. The response time of the system is however limited by the neutral gas conductance to approximately 0.5 s. Therefore, the KT5P values shown in the figure are averaged over time intervals of 0.5 s, which is not an issue for the comparison, since the TOFOR results are obtained with a lower time resolution than this. The orange bands show the  $\pm 1\sigma$  standard deviation in the averaged KT5P values.

## 5. Discussion

The fuel ion ratios measured by TOFOR and KT5P are to a large degree consistent, however, there are a number of differences between the two shown in figure 6 for the D(T) plasmas (JPN 98043 and 98044) and figure 7 for the T(D) plasmas (JPN 99093 and 99134). For 98043 and 98044 the first

**Table 1.** Time intervals and corresponding fuel ion ratios measured by TOFOR for D(T) plasmas corresponding to (a) JPN 98043 and (b) 98044.

| (a)          |   |
|--------------|---|
| Interval (s) | $\frac{n_{\text{T}}}{n_{\text{T}}+n_{\text{D}}} (\%)$ |
| 7–8          | 0.22 (3)  |
| 8–9          | 0.19 (3)  |
| 9–10         | 0.15 (2)  |
| 10–11        | 0.59 (5)  |
| 11–12        | 1.37 (12)   |
| 12–13        | 1.93 (17)   |
| 13–14        | 1.74 (14)   |
| 14–15        | 1.45 (14)   |
| 15–16        | 1.13 (16)   |
| (b)          |   |
| Interval (s) | $\frac{n_{\text{T}}}{n_{\text{T}}+n_{\text{D}}} (\%)$ |
| 7–8          | 0.15 (2)  |
| 8–9          | 0.20 (3)  |
| 9–10         | 0.24 (3)  |
| 10–11        | 0.94 (8)  |
| 11–12        | 1.70 (16)   |
| 12–13        | 2.02 (18)   |
| 13–14        | 2.09 (20)   |
| 14–15        | 1.50 (12)   |
| 15–16        | 1.33 (13)   |

**Table 2.** Time intervals and corresponding fuel ion ratios measured by TOFOR for T(D) plasmas corresponding to (a) JPN 99093 and (b) 99134.

| (a)          |   |
|--------------|---|
| Interval (s) | $\frac{n_{\text{T}}}{n_{\text{T}}+n_{\text{D}}} (\%)$ |
| 11–13        | 95.53 (36)  |
| 13–15        | 96.05 (27)  |
| 15–16        | 96.30 (29)  |
| 16–17        | 96.27 (26)  |
| 17–18        | 96.05 (28)  |
| 18–19        | 95.81 (37)  |
| (b)          |   |
| Interval (s) | $\frac{n_{\text{T}}}{n_{\text{T}}+n_{\text{D}}} (\%)$ |
| 12–13        | 96.43 (56)  |
| 13–14        | 96.93 (30)  |
| 14–15        | 96.73 (21)  |
| 15–16        | 96.84 (17)  |
| 16–17        | 96.86 (53)  |
| 17–18        | 96.79 (18)  |

three points disagree with KT5P within the given uncertainties. However, after a recent upgrade in preparation for DTE2 [14], KT5P reached a lower detection limit of T concentrations on the level of 1%, which is close to the first three points according to the TOFOR measurement. Further, the measured concentration, derived from fitting the optical spectra from the Penning gauge, will stay in the range of 0%–1% even when no T is present [15]. The TOFOR and KT5P measurements

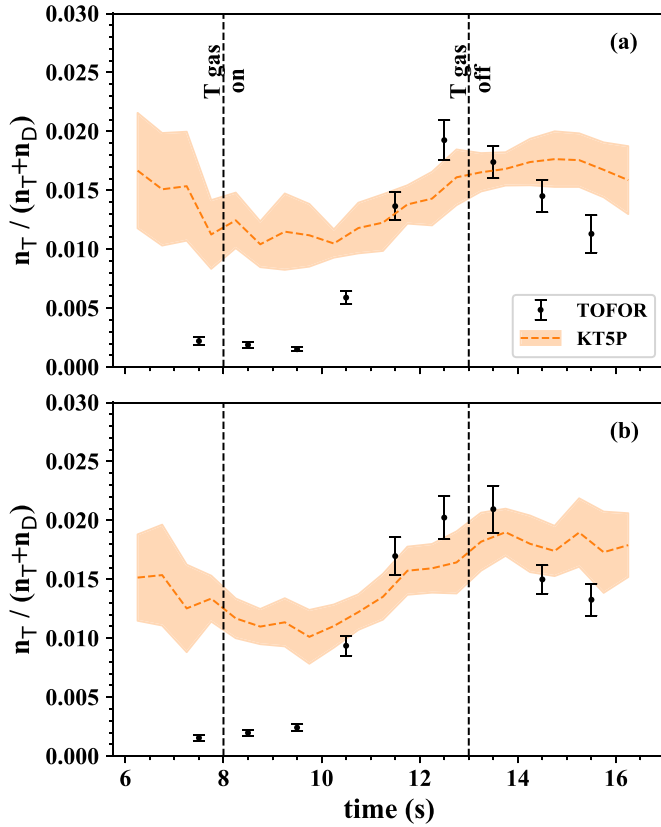


**Figure 6.** Fuel ion ratios averaged over a number of time intervals for (a) JPN 98043 and (b) JPN 98044, measured by TOFOR (black points) and KT5P (orange dashed line) including  $\pm 1\sigma$  statistical uncertainties (orange band).

agree within the given uncertainties for the points after 11 s at which the T concentration is on the level of 2%. From the two examples shown in figure 4, the increase of the DT peak amplitude between the two panels is reflected in the fuel ion ratios in figure 6, showing the corresponding expected increase in the T concentration between the first point (7–8 s) and the sixth point (12–13 s). The increase in T concentration can be attributed to the T gas puffing between 8 and 13 s. A significant increase in the T concentration is detected by TOFOR around 2.5 s after the T gas valves are opened. A similar decrease in T concentration is subsequently detected approximately 1.5 s after the T gas valves have closed. Given the TOFOR sight-line through the plasma core, our measurements suggest that it took approximately two seconds for a significant amount of the tritium to reach the plasma core. A similar observation is made by the total neutron rate shown in the top left panel of figure 1; approximately 2 s after the T gas is switched on there is a significant increase in the neutron rate. The main contribution to this time delay comes from the transport of gas from the tritium reservoir through the pipework to the torus. In the case of 99093 and 99134 (figure 7), the KT5P and TOFOR measurements follow similar trends. There is however a consistent vertical offset (more prominent in the upper panel) between the two systems throughout the discharge. A similar observation was made in an analysis of the JET DTE1 experiment from 1997 comparing data from the magnetic proton

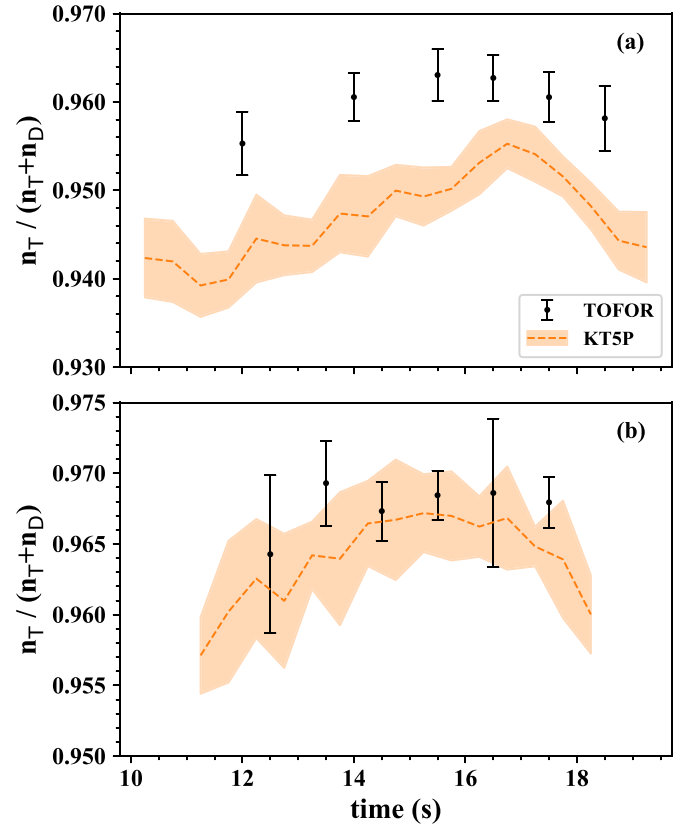


**Figure 7.** Fuel ion ratios averaged over a number of time intervals for (a) JPN 99093 and (b) JPN 99134 measured by TOFOR (black points) and KT5P (orange dashed line) including  $\pm 1\sigma$  statistical uncertainties (orange band).

recoil spectrometer and KT5P [5]. At that time, the difference between the two diagnostics was substantially larger than the results in this paper. The plasma in 99093 and 99134 consist to a large degree of  $^1\text{H}$  and T. Tritium NBI and H gas puffing was employed throughout the discharges, therefore, any D present in the tokamak comes solely from residual deuterium in the walls from previous experiments. As is argued in [5], it is thus possible that KT5P, which samples the sub-divertor region, measures a higher concentration of D, picked up from the tokamak walls, divertor gas exhaust ducts leading to the Penning gauge, or from deuterium trapped in the Penning gauge itself. Contributions of D from the walls will not affect TOFOR to the same degree since TOFOR's line-of-sight goes through the plasma core. Due to the centrally peaked neutron emissivity profile, the wall deuterium is only noticeable once it has penetrated to the central region of the plasma.

An important limitation of TOFOR's ability to measure the fuel ion ratio lies in the possibility to discern the DD peak (or TT continuum) among a tail of energy degraded DT neutrons originating from e.g. multiple scattering in the detector elements (this is taken into account in the instrumental response function) and in the JET machine materials (this is included in the scatter component of the fitting procedure). Further, the count rate dependent background due to random coincidences limits the peak visibility. In the DTE2 experimental campaign of high-performance DT discharges at JET

conducted during late 2021, there is a possibility to investigate the limits of  $n_T/(n_T + n_D)$  at which the analysis/method presented in this paper is possible using TOFOR. Such investigations are of further interest for future neutron spectroscopy efforts at, for example, ITER where there are plans to construct a high-resolution neutron spectrometer (HRNS) consisting of several neutron detection concepts, one of which may be a TOFOR-like spectrometer. The main purpose of such a TOF spectrometer would be to measure 2.5 MeV neutrons during pure D operations as well as the 14 MeV contribution of neutrons from tritium production associated with the DD reaction. In addition, measurements can also contribute in D(T) and T(D) scenarios, as shown here. The lessons learned regarding the possibilities and limitations identified for TOFOR in determining the fuel ion ratio, or other relevant plasma parameters, are valuable for the design of a future HRNS.

## 6. Conclusions

A method for measuring the fuel ion ratio for plasmas with low ( $n_T/(n_T + n_D) \sim 2\%$ ) and high ( $n_T/(n_T + n_D) \sim 96\%$ ) concentrations of tritium at JET is presented. As opposed to previous measurements of the fuel ion ratio using neutron spectrometry, we have shown that the continuum of neutron energies from the TT reaction can be employed in the determination of  $n_T/n_D$  for T(D) plasmas. Further, we have demonstrated the first use of a forward TOF neutron spectrometer for determining the fuel ion ratio. The method is applied to several plasma discharges in the JET experimental campaigns of 2020 and 2021. By fitting the different neutron TOF (energy) components in the measured TOF spectrum, it is possible to estimate  $n_T/n_D$  by determining the ratio of the reaction rates for reactions between different fuel ion populations. The presented results are consistent with the JET Penning gauge diagnostic KT5P in the limits at which KT5P is expected to provide reliable fuel ion estimates (typically for  $n_T/(n_T + n_D) > 1\%$ ). At high T concentrations, TOFOR's estimate is consistently higher than KT5P, which is likely due to a tendency of KT5P to measure an additional D contribution from the tokamak walls and divertor.

## Data availability statement

The data that support the findings of this study are available upon reasonable request from the authors.

## Acknowledgments

This work has been carried out within the framework of the EUROfusion Consortium and has received funding from the Euratom research and training programme 2014–2018 and 2019–2020 under Grant Agreement No. 633053. The views

and opinions expressed herein do not necessarily reflect those of the European Commission.

## ORCID iDs

B Eriksson  <https://orcid.org/0000-0002-7814-435X>  
 G Ericsson  <https://orcid.org/0000-0001-8530-4895>  
 J Eriksson  <https://orcid.org/0000-0002-0892-3358>  
 A Hjalmarsson  <https://orcid.org/0000-0002-3343-5591>  
 I S Carvalho  <https://orcid.org/0000-0002-2458-8377>  
 I Jezu  <https://orcid.org/0000-0001-8567-3228>  
 E Delabie  <https://orcid.org/0000-0001-9834-874X>

## References

- [1] Korsholm S B *et al* 2010 Development of novel fuel ion ratio diagnostic techniques *Rev. Sci. Instrum.* **81** 10D323
- [2] Stejner M *et al* 2012 The prospect for fuel ion ratio measurements in ITER by collective Thomson scattering *Nucl. Fusion* **52** 023011
- [3] Ericsson G *et al* 2010 Neutron spectroscopy as a fuel ion ratio diagnostic: lessons from JET and prospects for ITER *Rev. Sci. Instrum.* **81** 10D324
- [4] Hellesen C, Eriksson J, Conroy S, Ericsson G, Skiba M and Weiszflog M (JET-EFDA Contributors) 2012 Fuel ion ratio measurements in reactor relevant neutral beam heated fusion plasmas *Rev. Sci. Instrum.* **83** 10D916
- [5] Hellesen C *et al* 2015 Fuel ion ratio determination in NBI heated deuterium tritium fusion plasmas at JET using neutron emission spectrometry *Nucl. Fusion* **55** 023005
- [6] Johnson M G *et al* 2008 The 2.5-MeV neutron time-of-flight spectrometer TOFOR for experiments at JET *Nucl. Instrum. Methods Phys. Res. A* **591** 417–30
- [7] Sperduti A, Ceconello M, Conroy S, Eriksson J, Kirov K and Giacomelli L (JET Contributors) 2021 Plasma position measurement with collimated neutron flux monitor diagnostics on JET *Fusion Eng. Des.* **168** 112597
- [8] Jarvis O 1994 Neutron measurement techniques for tokamak plasmas *Plasma Phys. Control. Fusion* **36** 209
- [9] Stix T H 1975 Fast-wave heating of a two-component plasma *Nucl. Fusion* **15** 737
- [10] Spitzer L 1962 *Physics of Fully Ionized Gases* 2nd edn (New York: Interscience)
- [11] Johnson M G *et al* 2010 Modelling and TOFOR measurements of scattered neutrons at JET *Plasma Phys. Control. Fusion* **52** 085002
- [12] Hillis D, Klepper C, Von Hellermann M, Ehrenberg J, Finken K and Mank G 1997 Deuterium-tritium concentration measurements in the divertor of a tokamak via a modified Penning gauge *Fusion Eng. Des.* **34** 347–51
- [13] Hillis D, Morgan P, Ehrenberg J, Groth M, Stamp M, Von Hellermann M and Kumar V 1999 Tritium concentration measurements in the Joint European Torus divertor by optical spectroscopy of a Penning discharge *Rev. Sci. Instrum.* **70** 359–62
- [14] Kruezi U, Jezu I, Sergienko G, Klepper C C, Delabie E, Vartanian S and Widdowson A 2020 Neutral gas analysis for JET DT operation *J. Instrum.* **15** C01032
- [15] Klepper C *et al* 2019 Sub-divertor fuel isotopic content detection limit for JET and its impact on ICRF core heating and DTE2 operation *Nucl. Fusion* **60** 016021